Density Functional Study of Catalytic Silane Alcoholysis at a $[Fe(Cp)(CO)(PR_3)]^+$ Center†

Michael Bühl* and Frank T. Mauschick

Max-Planck-Institut für Kohlenforschung, Kaiser-Wilhelm-Platz 1, D-45470 Mülheim an der Ruhr, Germany

Received October 24, 2002

Catalytic conversion of MeOH and SiH_4 to $MeOSiH_3$ and H_2 at a $[Fe(Cp)(CO)(PR_3)]^+$ center was studied computationally at a gradient-corrected level of density functional theory (BP86). Intermediates and transition states for R′ = H and Ph were characterized along the catalytic cycle, the rate-determining step of which is indicated to be H_2 dissociation from $[Fe(Cp)(CO)(PR_3)(H_2)]^+$, in accord with a mechanistic study for higher substituted substrates (Brookhart, et al. *J. Mol. Catal. A* **1998**, *130*, 107). For the model catalyst (R = H), introduction of $SiMe_3$, NMe_2, COMe, NO_2, CN, or Cl substituents at the Cp ring decreases the rate-determining barrier (up to 6 kcal/mol for NMe_2). A loose correlation is found between these barriers and $\delta(^{57}Fe)$ values computed for the correspondingly derivatized precursor models $Fe(C_5H_4X)(CO)(PH_3)Me$. In the transient, free $[Fe(C_5H_4X)(CO)(PPh_3)]^+$ complex, there can be competition between the substituent X and a phenyl group of the PPh_3 ligand for a hemilabile intramolecular coordination to iron. Modification of the phosphine is thus expected to open further possibilities for tuning the catalyst properties and activities.

Introduction

Protecting group techniques are basic tools in preparative chemistry. The quest for ever more selective transformations entails the need for protection of functional groups under mild conditions. For example, the classic way to transform an alcoholic group into a silyl ether by reaction with a chlorosilane (eq 1) requires strongly basic conditions, which is not tolerated if other base-sensitive groups are present. Therefore, alternative strategies have been developed, for instance the reaction with silanes catalyzed by a plethora of transition metal complexes (eq 2). [1−4]

$$R{-}OH + R'_3Si{-}Cl \xrightarrow[-HCl]{Base} R{-}O{-}SiR'_3 \qquad (1)$$

$$R{-}OH + R'_3Si{-}H \xrightarrow[-H_2]{Cat.} R{-}O{-}SiR'_3 \qquad (2)$$

Research efforts are being devoted to overcome problems of side reactions, such as hydrosilylation if double bonds are present, to prevent catalyst deactivation, and to improve the catalytic activity of the metal complexes. In the latter respect, very promising results have been obtained for a cationic Ir complex,[5] as compared to the more commonly used neutral species. With these observations in mind, Brookhart and co-workers have recently undertaken a detailed mechanistic study of silane alcoholysis at a $[(Cp)(CO)(PPh_3)Fe]^+$ center.[2] Rapid deactivation of the catalyst occurs with ethanol as substrate, but phenol reacts continuously with respectable turnover numbers up to 80 min^{-1}. Key intermediates have been observed via NMR spectroscopy, which has allowed to deduce a detailed picture of the catalytic cycle. A simplified form of this cycle is given in Scheme 1.

Protonation of the catalyst precursor **1a** using $[H(OEt_2)_2]^+[(3,5\text{-}(CF_3)\text{-}C_6H_4)_4B]^-$ and reaction with excess silane affords the silane complex **A**, which transfers the silyl group to the alcohol, affording the dihydrogen complex **C**, presumably via the transient hydride **B**. Under catalytic conditions, i.e., with phenol as substrate, displacement of the H_2 ligand in **C** by silane appears to be the rate-determining step.[2] In the first part of this paper we present a computational study of a model reaction (R = R′ = H, R″ = Me), which confirms this mechanism, subject to a minor revision.

In the second part of this paper we study substituent effects on the barrier of the rate-determining step in order to predict how the activity of the actual catalyst could be enhanced. In the third part, we extend our mechanistic studies to the real catalytic center (R′ = Ph, Scheme 1), to test the reliability of the predictions for the model system.

† Dedicated to Prof. M. Reetz on the occasion of his 60th birthday.

* Corresponding author. Fax: Int. code + (0)208-306 2996. E-mail: buehl@mpi-muelheim.mpg.de.

(1) For reviews see: (a) Lukevics, E.; Dzintara, M. *J. Organomet. Chem.* **1985**, *295*, 265−315. (b) Corey, J. Y. In *Advances in Silicon Chemistry*; Larson, G., Ed.; JAI Press: Greenwich, CT, 1991; pp 327−387.

(2) Chang, S.; Scharrer, E.; Brookhart, M. *J. Mol. Catal. A* **1998**, *130*, 107−119.

(3) For recent examples, see e.g.: (a) Ito, H.; Ishizuka, T.; Okumura, T.; Yamanaka, H.; Tateiwa, J.-I.; Sonada, M.; Hosomi, A. *J. Organomet. Chem.* **1999**, *574*, 102−106. (b) Fang, X.; Huhmann-Vincent, J.; Scott, B. L. Kubas, G. J. *J. Organomet. Chem.* **2000**, *609*, 95−103. (c) Chung, M.-K.; Ferguson, G.; Robertson, V.; Schlaf, M. *Can. J. Chem.* **2001**, *79*, 949−957. (d) Sudhakar, S.; Luh, T. Y. *J. Org. Chem.* **2002**, *67*, 6860−6862.

(4) For transition-metal-free systems see: (a) Blackwell, J. M.; Foster, K. L.; Beck, V. H.; Piers, W. E. *Organometallics* **1999**, *64*, 4887−4892. (b) Zacuto, M. J.; O'Malley, S. J.; Leighton, J. L. *J. Am. Chem. Soc.* **2002**, *124*, 7890−7891.

(5) Luo, X.; Crabtree, R. H. *J. Am. Chem. Soc.* **1989**, *111*, 2527−2535.

10.1021/om020890m CCC: $25.00
Publication on Web 02/22/2003

Scheme 1

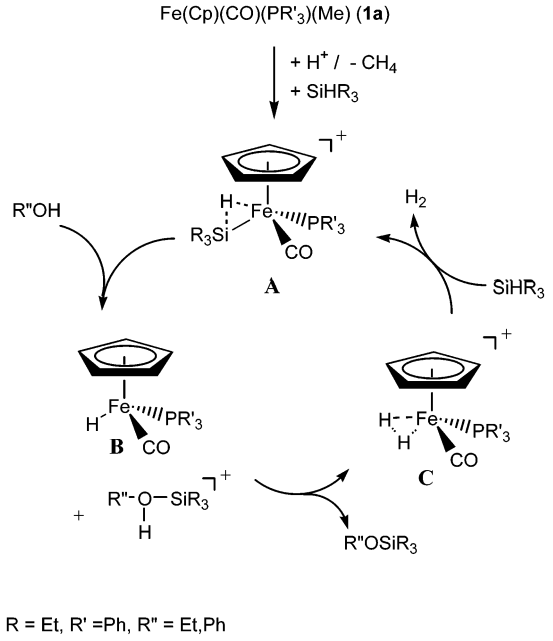

Computational Details

Stationary points were optimized at the BP86/AE1 level, i.e., employing the exchange and correlation functionals of Becke[6] and Perdew,[7] respectively, together with a fine integration grid (75 radial shells with 302 angular points per shell), the augmented Wachters' basis[8] on Fe (8s7p4d, full contraction scheme 62111111/3311111/3111), and 6-31G* basis on all other elements.[9] This and comparable DFT levels have proven quite successful for transition metal compounds and are well suited for the description of structures, energies, barriers, etc.[10] The nature of the stationary points was verified by computations of the harmonic frequencies at that level. Transition states were characterized by a single imaginary frequency, and visual inspection of the corresponding vibrational modes ensured that the desired minima are connected. In cases of doubt, the key parts of the intrinsic reaction coordinate were followed. The computed harmonic frequencies were used to evaluate zero-point energies (ZPEs) and enthalpic and entropic corrections at 300 K. Energies are reported at the BP86/AE1 + ZPE level (denoted ΔE + ZPE); in addition, the estimated ΔG values are given as well. For most of the larger complexes, a somewhat smaller basis set was used on the C atoms of the PPh_3 moiety, where polarization functions were only given to the ipso-C atom, the others being described by the 6-31G basis (denoted AE1′). These computations were performed with the Gaussian 98 program.[11]

In addition, selected PPh_3 complexes were optimized at the BP86 level using the full AE1 basis set and the RI (resolution of identity) approximation as implemented[12] in TURBOMOLE,[13] together with a medium-sized grid (grid 3).[14] These optimizations were effected using ChemShell[15] and a suitable combination of Cartesian and hybrid delocalized internal coordinates.[16] Transition states were fully optimized and characterized by numerical evaluation of the harmonic vibrational frequencies, which were also used for zero-point correction. All optimized geometries are supplied as Supporting Information.

Magnetic shieldings were computed for BB86/AE1 geometries employing the B3LYP[17] hybrid functional, together with basis II′, which consists of the same Wachters' basis set on Fe as described above, a contracted (5s4p1d) Huzinaga basis on C and O, a contracted (7s6p2d) Huzinaga basis on P, and a double-ζ basis (2s) on H.[18] This particular combination of density functionals and basis sets has proven to perform well for the computation of ^{57}Fe chemical shifts.[19] The theoretical $\delta(^{57}Fe)$ values were referenced to $Fe(CO)_5$, for which a magnetic shielding of −2903 ppm is obtained at the same level.

Results and Discussion

1. Catalytic Model Cycle. The first steps corresponding to the transformation **A** → **B** → **C** in Scheme 1 are depicted in Figure 1 for the model system. Salient energies and thermodynamic data are collected in Table 1. The starting point for the computations was the silane complex **2**, the optimized structure of which displays the characteristics of this type of complexes, that is, side-on coordination with a significantly elongated Si−H bond.[20,21] The BP86/AE1 structure of **2** is very similar to that of closely related neutral $Mn(C_5H_4Me)(CO)(PMe_3)(H-SiHPh_2)$ in the solid.[22]

To proceed to the hydride **B** in Scheme 1, complex **2** has to transfer a SiH_3 moiety to the alcoholic substrate. When methanol, as a model for the latter, was approached to the Si center of **2** in a "backside" fashion (i.e., trans to the metal fragment), complex **3** was obtained without any barrier. On going from **2** to **3**, the Fe−Si bond is practically cleaved. The SiH_3 moiety in **3** is nearly planar, and the overall coordination geometry about Si is close to a trigonal bipyramid (H−SiH_3−O angle 163°). Such pentacoordinate structures

(6) Becke, A. D. *Phys. Rev. A* **1988**, *38*, 3098−3100.
(7) Perdew, J. P. *Phys. Rev. B* **1986**, *33*, 8822−8824. Perdew, J. P. *Phys. Rev. B* **1986**, *34*, 7406.
(8) (a) Wachters, A. J. H. *J. Chem. Phys.* **1970**, *52*, 1033−1036. (b) Hay, P. J. *J. Chem. Phys.* **1977**, *66*, 4377−4384.
(9) (a) Hehre, W. J.; Ditchfield, R.; Pople, J. A. *J. Chem. Phys.* **1972**, *56*, 2257−2261. (b) Hariharan, P. C.; Pople, J. A. *Theor. Chim. Acta* **1973**, *28*, 213−222.
(10) See for instance: Koch, W.; Holthausen, M. C. *A Chemist's Guide to Density Functional Theory*; Wiley-VCH: Weinheim, 2000, and the extensive bibliography therein.
(11) Frisch, M. J.; Trucks, G. W.; Schlegel, H. B.; Scuseria, G. E.; Robb, M. A.; Cheeseman, J. R.; Zakrzewski, V. G.; Montgomery, J. A.; Stratman, R. E.; Burant, J. C.; Dapprich, S.; Millam, J. M.; Daniels, A. D.; Kudin, K. N.; Strain, M. C.; Farkas, O.; Tomasi, J.; Barone, V.; Cossi, M.; Cammi, R.; Mennucci, B.; Pomelli, C.; Adamo, C.; Clifford, S.; Ochterski, J.; Petersson, G. A.; Ayala, P. Y.; Cui, Q.; Morokuma, K.; Malick, D. K.; Rabuck, A. D.; Raghavachari, K.; Foresman, J. B.; Cioslowski, J.; Ortiz, J. V.; Baboul, A. G.; Stefanov, B. B.; Liu, C.; Liashenko, A.; Piskorz, P.; Komaromi, I.; Gomperts, R.; Martin, R. L.; Fox, D. J.; Keith, T.; Al-Laham, M. A.; Peng, C. Y.; Nanayakkara, A.; Gonzalez, C.; Challacombe, M.; Gill, P. M. W.; Johnson, B. G.; Chen, W.; Wong, M. W.; Andres, J. L.; Gonzales, C.; Head-Gordon, M.; Replogle, E. S.; Pople, J. A. *Gaussian 98*; Gaussian, Inc.: Pittsburgh, PA, 1998.
(12) (a) Eichkorn, K.; Treutler, O.; Öhm, H.; Häser, M.; Ahlrichs, R. *Chem Phys. Lett.* **1995**, *240*, 283−289. (b) Eichkorn, K.; Treutler, O.; Öhm, H.; Häser, M.; Ahlrichs, R. *Chem Phys. Lett.* **1995**, *242*, 652−660.
(13) Ahlrichs, R.; Bär, M.; Häser, M.; Horn, H.; Kölmel, C. *Chem. Phys. Lett.* **1989**, *162*, 165−169.
(14) Treutler, O.; Ahlrichs, R. *J. Chem. Phys.* **1995**, *102*, 346−354.
(15) Sherwood, P.; deVries, A. H. *ChemShell−A Shell for Computational Chemistry*; CCLRC Daresbury Laboratory, 1999; see http://www.dl.ac.uk.
(16) Billeter, S. R.; Turner, A. J.; Thiel, W. *Phys. Chem. Chem. Phys.* **2000**, *2*, 2177−2186.
(17) (a) Becke, A. D. *J. Chem. Phys.* **1993**, *98*, 5648−5652. (b) Lee, C.; Yang, W.; Parr, R. G. *Phys. Rev. B* **1988**, *37*, 785−789.
(18) Kutzelnigg, W.; Fleischer, U.; Schindler, M. In *NMR Basic Principles and Progress*; Springer-Verlag: Berlin, 1990; Vol. 23, pp 165−262.
(19) Bühl, M. *Chem. Phys. Lett.* **1997**, *267*, 251−257.
(20) For a recent review, see: Lin, Z. *Chem. Soc. Rev.* **2002**, *31*, 239−245.
(21) Metal−silane bonding has recently attracted interest in context with nonclassical interligand interactions, see e.g.: Nikonov, G. I. *Angew. Chem. Int. Ed.* **2001**, *40*, 3353−3355.
(22) Schubert, U.; Scholz, G.; Müller, J.; Ackermann, K.; Worle, B.; Stansfield, R. F. D. *J. Organomet. Chem.* **1986**, *306*, 303−326.

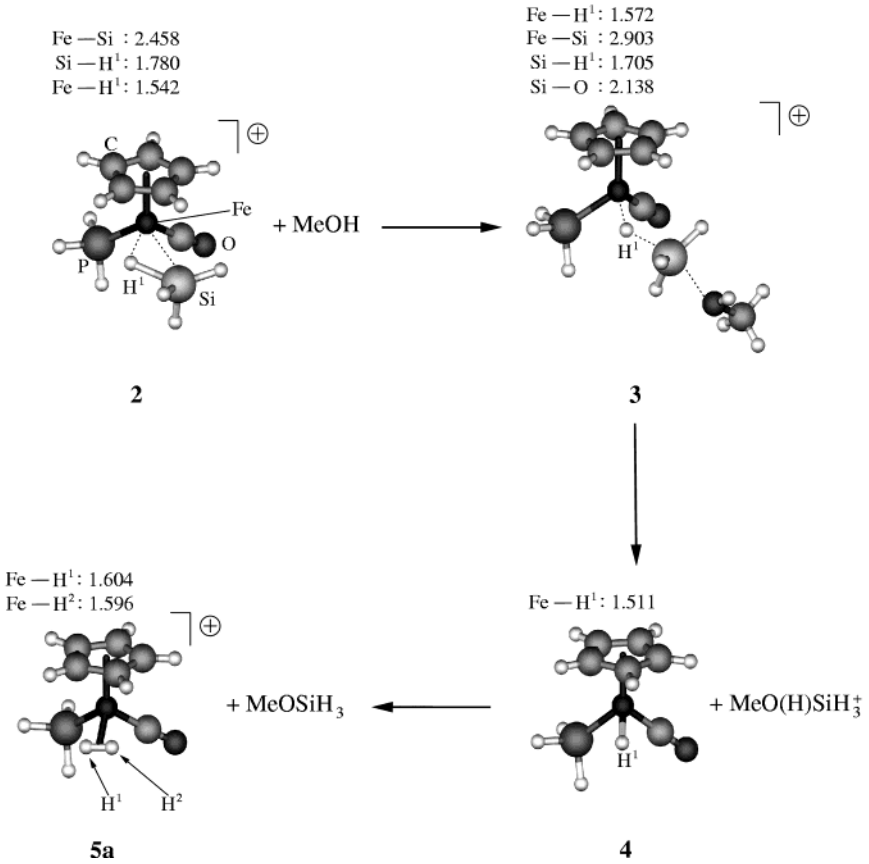

Figure 1. Dissociative pathway for product formation in the catalytic model cycle (key distances are given in Å (BP86/AE1 level)).

Table 1. Relative Energies (kcal/mol, BP86/AE1 level) of Stationary Points in Catalytic Silane Alcoholysis at the Catalytic Center Model (PH_3 as Phosphine); {Fe} = [Fe(Cp)(CO)(PH_3)]$^+$

complex	ΔE	ΔE+ZPE[a]	ΔH[b]	ΔG[b]
{Fe}(SiH_4)(**2**) + SiH_4 + MeOH	0.0	0.0	0.0	0.0
{Fe}($HSiH_3$···OHMe) (**3**) + SiH_4	−12.2	−10.6	−10.3	−1.3
Fe(Cp)(CO)(PH_3)H (**4**) + SiH_4 + $MeO(H)SiH_3^+$	19.4	19.6	19.4	17.7
{Fe}(SiH_4)(HOMe)‡ (**TS5a**) + SiH_4	2.7	3.8	3.4	14.3
{Fe}(H_2) (**5a**) + $MeOSiH_3$ + SiH_4	−11.2	−12.4	−12.7	−13.5
{Fe}(H_2)(SiH_4)‡ (**TS5a2**) + $MeOSiH_3$	12.6	8.5	9.8	13.0
{Fe} (**6a**) + H_2 + $MeOSiH_3$ + SiH_4	15.5	9.4	11.1	0.6
{Fe}(SiH_4)(**2**) + H_2 + $MeOSiH_3$	−15.0	−18.1	−17.3	−16.2

[a] Including zero-point energies. [b] Thermodynamic corrections at 300 K from BP86/AE1 harmonic frequencies.

have also been found computationally for related systems without transition metals.[23] The association energy of **2** and MeOH is notable on the potential energy surface (PES), −10.6 kcal/mol (including ZPE), but is reduced—in absolute terms—to −6.5 kcal/mol upon correction for basis set superposition error (BSSE). Entropy further disfavors formation of this associate (ΔG = −1.3 kcal/mol, Table 1), and it seems thus unlikely that **3** would be significantly populated under real conditions (see also section 3).

Dissociation of the protonated silyl ether from **3** affords the neutral hydride complex **4**. Taking the H···Si separation as reaction coordinate, no transition state for this transformation could be found. Actually, much of the positive charge of the metal complex is already transferred to the nascent silyl ether moiety in **3**, as natural population analysis (NPA)[24] affords a total charge of +0.55 for this fragment. Dissociation costs a lot of energy, more than 30 kcal/mol relative to **3**, and on the free energy surface, the reaction

$$\mathbf{2} + \mathrm{MeOH} \rightarrow \mathbf{4} + \mathrm{MeO(H)SiH_3^+} \qquad (3)$$

is quite endergonic with ΔG = +17.7 kcal/mol (Table 1). The driving force for reprotonation of **4** by $MeO(H)SiH_3^+$ is large and serves to stabilize the products, dihydrogen complex **5a** and $MeOSiH_3$, by −12.4 kcal/mol relative to the reactants (ΔG = −13.5 kcal). As an alternative to the backside attack just described, we also investigated the possibility of a "frontside" attack, where the methanol approaches the Si center from the same side as the metal fragment. Intuitively, one would consider such a arrangement to be less favorable due to steric congestion. However, we could locate a low-lying transition structure (**TS25a**, Figure 2), which leads directly to **5a** (or rather, to a slightly more stable ion-dipole complex **5a**·$OMeSiH_3$, not shown), without occurrence of a free hydride complex. Even though **TS25a** is an early transition state, as judged by the small energy barrier on the PES (3.8 kcal/mol with respect to **2** + MeOH), the Fe···Si contact is already all

(23) Olsson, L.; Ottosson, C.-H.; Cremer, D. *J. Am. Chem. Soc.* **1995**, *117*, 7460−7479.

(24) Reed, A. E.; Curtiss, L. A.; Weinhold, F. *Chem. Rev.* **1988**, *88*, 899−926.

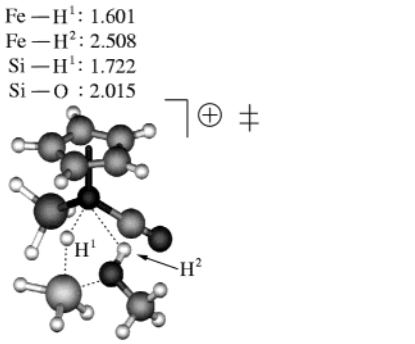

2 ⟶ 5a

TS25a

Figure 2. Transition structure for associative product formation (key BP86/AE1 distances in Å).

but broken. Due to partial loss of conformational flexibility in the pseudo-five-membered ring, and because of its associative nature, **TS25a** is disfavored entropically. However, the estimated barrier on the free energy surface, $\Delta G^{\ddagger} = 14.3$ kcal/mol, is significantly lower than the highest point on the backside pathway (via **4**, $\Delta G = 17.7$ kcal/mol, Table 1). While this difference may change for the actual, bulky substituents (see, however, section 3), this result strongly suggests that direct transformation of the silane complex to the dihydrogen complex is possible and can occur without formation of a transient hydride **B**. The observation of the latter in the NMR spectra can be attributed to side reactions, e.g., to the equilibrium

$$\mathbf{C} + \mathrm{R{-}OH} \rightleftharpoons \mathbf{B} + \mathrm{R{-}OH_2^+} \qquad (4)$$

which, apparently, has been found to be shifted to the left and right side for R = Et and Ph, respectively.[2]

Another factor that, under experimental conditions, could favor formation of the hydride **B** from **A** (or **4** from **2** in the model reaction, eq 3) is stabilization of the protonated silyl ether by the protic solvent, excess alcohol.[25] For a definite conclusion, such solvent effects would have to be included explicitly in the computations. This was not deemed necessary since this step most likely is not the rate-determining one (see below).

It is not uncommon for transition metal dihydrogen complexes[26] to be in tautomeric equilibrium with the corresponding dihydride.[27] Cationic **C** has been shown to exist exclusively as a dihydrogen complex.[28] Consistent with this observation, an attempted optimiziation of a *cis*-$[Fe(Cp)(CO)(PH_3)(H)_2]^+$ complex collapsed to the dihydrogen complex **5a**. The corresponding *trans*-dihydride could be located, but was found 4.0 kcal/mol above isomeric **5a** (ΔE + ZPE).The catalytic cycle is completed by displacement of H_2 in **5a** by fresh silane. This reaction can either occur in an associative fashion, via **TS5a2**, or follow a dissociative mechanism, via the unsaturated intermediate **6a** (Figure 3). Both pathways are almost isoenergetic on the PES, but are differentiated by entropy, which strongly favors dissociation. On the free energy surface, **6a** + H_2 are only 14.1 kcal/mol above the dihydrogen complex **5a** (Table 1). Both H_2 and SiH_4 addition to **6a** are barrierless on the PES,[29] which would suggest a facile displacement of H_2 by SiH_4 in **5a**, in particular since the overall reaction is exothermic:

$$\mathbf{5a} + SiH_4 \rightarrow \mathbf{2} + H_2,\ \Delta E + \mathrm{ZPE} = -5.7 \text{ kcal/mol}\ (\Delta G = -2.7 \text{ kcal/mol}) \qquad (5)$$

The high activity of $[IrH_2(THF)_2(PPh_3)_2]^+$ has been ascribed to the possibility that, after dissociation of the labile THF ligands, both reaction partners, alcohol and silane, can be coordinated to the metal at the same time.[5] It would be conceivable to achieve the same simultaneous coordination to the $[Fe(Cp)(CO)(PR'_3)]^+$ center, if an additional coordination site could be created by reducing the hapticity of the Cp ligand. For a number of cases this so-called ring slippage has been inferred experimentally[30] and confirmed computationally.[31] Despite extensive searches, no viable pathway involving such a ring slippage could be found for the model system under investigation. Stationary points of the type $[Fe(\eta^3\text{-}Cp)(CO)(PH_3)L_2]^+$, $L_2 = (SiH_4)(MeOH)$, $(SiH_4)(H_2)$, could not be located at all or were excessively high in energy.

From the results obtained so far we can conclude that the basic mechanism proposed for silane alcoholysis (Scheme 1) is confirmed computationally for the model system, with one addition: The transformation of **A** into **C** can take place either under formation of the transient free hydride **B** or in a single step circumventing this intermediate. According to the results for the model system in the gas phase, the latter pathway could be competitive, or even the preferred one.

Unfortunately, the rate-limiting step cannot be deduced unambiguously from this model study. Experimentally, H_2 displacement by silane appears to be rate-determining.[2] On the PES, this step indeed requires the highest activation energy. Enthalpic and entropic corrections, however, render formation of the H_2 complex and H_2 displacement from it almost isoenergetic (see values in parentheses in eqs 6 and 7):

	$\Delta E^{\ddagger}$ + ZPE	($\Delta G^{\ddagger}$) [kcal/mol]	
2 + MeOH → [**TS25a**]‡	3.8 (14.3)		(6)
5a → **6a** + H_2	21.8 (14.1)		(7)

Thus, for both alternatives virtually the same free activation energy is obtained. It must be noted, however,

(25) A smaller cation is usually solvated more strongly than a larger one. On the other hand, the observed equilibrium of eq 4 can also be shifted to the side with the larger cation, **C**.

(26) Heinekey, D. A.; Oldham, W. J., Jr. *Chem. Rev.* **1993**, *93*, 913−926.

(27) For recent examples see, e.g.: (a) Drouin, S. D.; Yap, G. P. A.; Fogg, D. E. *Inorg. Chem.* **2000**, *39*, 5412−5414. (b) Torres, L.; Moreno, M.; Lluch, J. M. *J. Phys. Chem. A* **2001**, *105*, 4676−4681. (c) Esteruelas, M. A.; García-Yebra, C.; Oliván, M.; Oñate, E.; Tajada, M. A. *Organometallics* **2002**, *21*, 1311−1314.

(28) Scharrer, E.; Chang, S.; Brookhart, M. *Organometallics* **1995**, *14*, 5686−5694.

(29) "Barrierless" here means that no extra activation in addition to the reaction energy is necessary. There could be, in principle, a barrier on the free energy surface, resulting from the increase of rotational and translational entropies upon dissociation; see e.g.: Woo, T. K.; Blöchl, P. E.; Ziegler, T. *J. Phys. Chem. A* **2000**, *104*, 121−129.

(30) E.g.: (a) Li, L.-N.; Rerek, M. E.; Basolo, F. *Organometallics* **1984**, *3*, 740−745. (b) Review: O'Connor, J. M.; Casey, C. P. *Chem. Rev.* **1987**, *87*, 307−318. (c) Simanko, W.; Tesch, S.; Sapunov, V. N.; Mereiter, K.; Schmid, R.; Kirchner, K.; Coddington, J.; Wherland, S. *Organometallics* **1998**, *17*, 5674−5688.

(31) E.g.: (a) Bühl, M. *Organometallics*, **1997**, *16*, 261−267. (b) Fan, H. J.; Hall, M. B. *Organometallics* **2001**, *20*, 5724−5730. (c) Calhorda, M. J.; Romão, C. C.; Veiros, L. F. *Chem. Eur. J.* **2002**, *8*, 868−875.

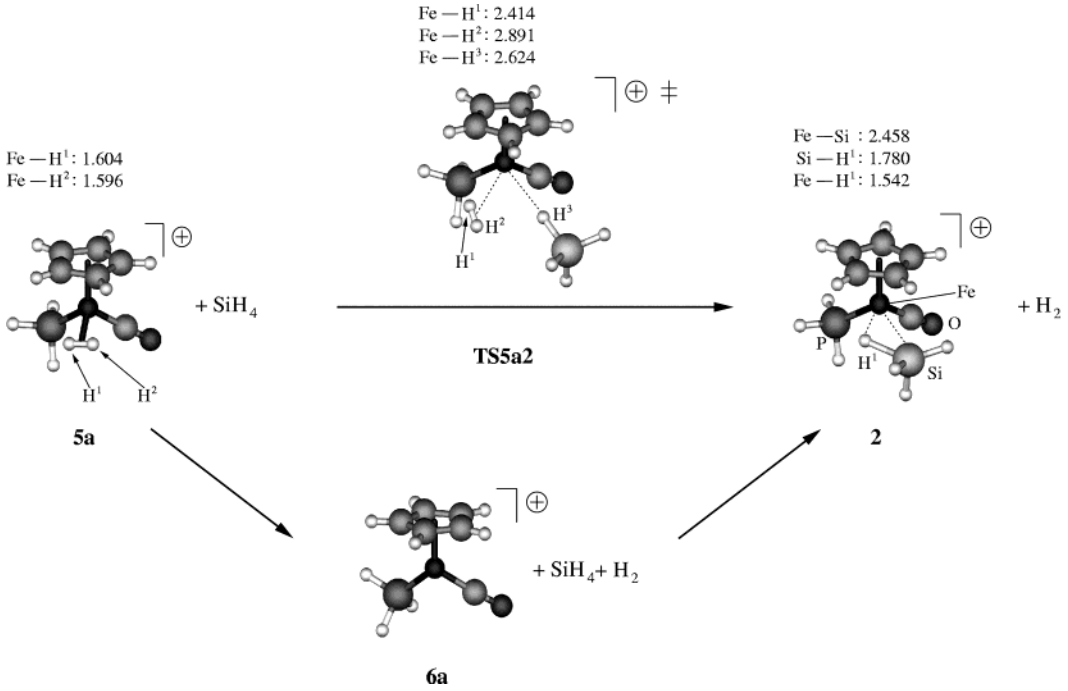

Figure 3. Regeneration of the model catalyst via associative (top) or dissociative pathways (bottom, key BP86/AE1 distances in Å).

that the computed entropies are only rough estimates based on the ideal-gas assumption. In particular when low vibrational modes are present, as in all of the iron complexes, the estimated entropies can be significantly overestimated. The actual free energies in eq 6 and eq 7 may thus be somewhat closer to the respective ΔE + ZPE values.

Even if both alternatives have the same free activation energy, it is quite likely that under actual catalytic conditions the first step (eq 6) would occur at a higher rate than the second (eq 7), simply because in the former the alcoholic substrate is present in a large excess. In summary, these arguments would tend to suggest that it is indeed H_2 dissociation that is rate-limiting, consistent with the experimental findings. Therefore this assumption will be our working hypothesis for the evaluation of substituent effects on the catalytic activity, which is discussed in the following section.

2. Substituent Effects. The electronic properties of the catalyst precursor **1A** can be modified by introducing substituents at the Cp ring. Both electron-withdrawing and -releasing substituents have been realized, and the concomitant steric and electronic effects are reflected in the ^{57}Fe chemical shifts,[32] which undergo variations of up to ca. 200 ppm for a series of derivatives of **1A** (see experimental δ values in Scheme 2).[33]

How would these substituents affect the catalytic activity in silane alcoholysis? To address this question, we have made the corresponding modifications to the

Scheme 2

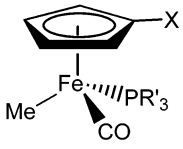

R′ = Ph			R′ = H
	X	$\delta(^{57}Fe)_{expt}$	X
1A	H	*1392*	**1a** H
1B	$SiMe_3$	*1421*	**1b** $SiMe_3$
1C	NEt_2	*1437*	**1c** NMe_2
1D	CO^iPr	*1580*	**1d** COMe
			1e NO_2
			1f CN
			1g Cl

stationary points of H_2 dissociation (eq 7), believed to be the rate-determining step in the catalytic model cycle. Because of the model character of this cycle, more remote bulky alkyl groups have been omitted (see entry R′ = H in Scheme 2 for the actual substituents employed in the computations), and other substituents not yet realized experimentally have been included. To find the most stable isomer of, respectively, **5b**−**g** and **6b**−**g**, each of the Cp hydrogen atoms in **5a** and **6a** was replaced by the corresponding substituent, followed by a full geometry optimization. For carbonyl, silyl, and nitro derivatives, the dissociation products (**6b, 6d**, and **6e**, respectively) are characterized by an intramolecular interaction between the iron atom and the substituent. Apparently, the energy gain due to the partial saturation of the electron deficiency at the metal is quite large and outweighs the strain induced by the deformations at the Cp ring, which are necessary to achieve this interaction (see the optimized geometries in Figure 4). The energetic separation between isomers with and without this interaction may serve as an estimate for the stabilization. For **6b**, **6d**, and **6e** the next highest minimum without the intramolecular contact is 7.1, 12.4, and 11.0 kcal/mol, respectively, above the isomers displayed in Figure 4 (BP86/AE1 level). As a consequence, the resulting H_2 dissociation energies are lower

(32) There has been a renaissance of ^{57}Fe NMR spectroscopy of late, see for instance: (a) Wrackmeyer, B.; Ayazi, A.; Maisel, H. E.; Herberhold, M. *J. Organomet. Chem*. **2001**, *630*, 263−265. (b) Wrackmeyer, B.; Maisel, H. E.; Herberhold, M. *Z. Naturforsch.* **2001**, *56b*, 1373−1375. (c) Wrackmeyer, B.; Tok, O. L.; Ayazi, A.; Hertel, F.; Herberhold, M. *Z. Naturforsch.* **2002**, *57b*, 305−308. For an earlier review see: (d) Benn, R. In *Transition Metal Nuclear Magnetic Resonance*; Pregosin, P. S., Ed.; Elsevier: Amsterdam, 1991; pp 102−142.

(33) Meier, E. J. M.; Koźmiński, W.; Linden, A.; Lustenberger, P.; von Philipsborn, W. *Organometallics* **1996**, *15*, 2469−2477.

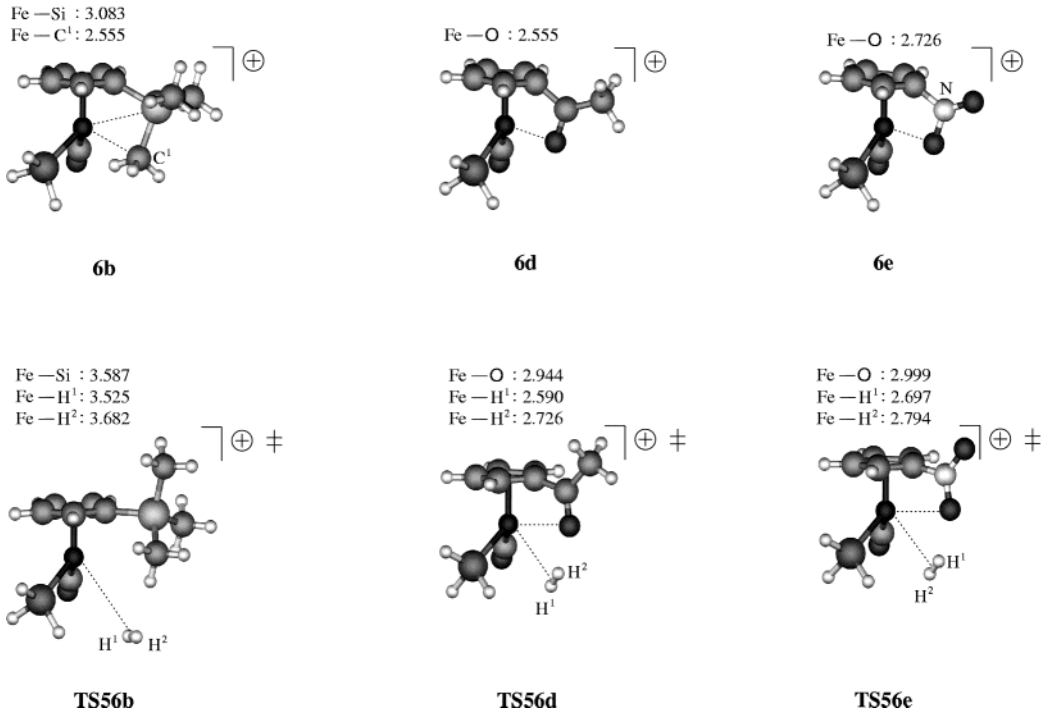

Figure 4. BP86/AE1 optimized reaction products (top) and transition states (bottom) for H_2 dissociation from the corresponding $[Fe(C_5H_4X)(CO)(PH_3)(H_2)]^+$ derivatives (**5x**). Note the intramolecular contacts in the products shown involving the substituents at the Cp rings (distances in Å).

Table 2. Substituent Effects on Reaction Energy and Activation Barrier of H_2 Dissociation from $[Fe(C_5H_4X)(CO)(PH_3)(H_2)]^+$ (5x)[a]

substituent X	**5x** → **6x** + H_2			**5x** → [**TS56x**]‡			**1x**
	ΔE	(+ZPE)	(ΔG)	$\Delta E^‡$	(+ZPE)	($\Delta G^‡$)	$\delta(^{57}Fe)$[b]
a H	26.7	(21.8)	(*14.1*)	26.7[c]	(21.8)[c]	(*14.1*)[c]	1364
b $SiMe_3$	19.6	(15.1)	(*9.1*)	25.2	(21.0)	(*18.6*)	1405
c NMe_2	20.3	(15.8)	(*8.6*)	20.3[c]	(15.8)[c]	(*8.6*)[c]	1620
d COMe	13.5	(9.1)	(*2.7*)	24.0	(20.8)	(*19.8*)	1453
e NO_2	15.3	(10.6)	(*4.3*)	25.0	(21.3)	(*19.6*)	1501
f CN	25.8	(21.0)	(*13.6*)	25.8[c]	(21.0)[c]	(*13.6*)[c]	1489
g Cl	22.9	(18.3)	(*10.9*)	22.9[c]	(18.3)[c]	(*10.9*)[c]	1366

[a] Energies are given in kcal/mol at the BP86/AE1 level (in parentheses: zero-point corrected values, in italics: estimated free energies at 300 K). In addition, B3LYP/II′ ^{57}Fe chemical shifts are given for corresponding catalyst precursor models, $Fe(C_5H_4X)(CO)(PH_3)Me$ (**1x**). [b] In ppm relative to $Fe(CO)_5$. [c] No barrier on the PES; therefore $\Delta E = \Delta E^‡$.

by a similar amount, relative to the parent **5a** (compare the first entry for **a** with that of **b**, **d**, and **e** in Table 2). In the course of the dissociation, however, H_2 has to move quite far away from the metal before the intramolecular stabilization can set in. Therefore, this should be an activated process. We have located the corresponding transition states, **TS56b, TS56d**, and **TS56e**, which are included in Figure 4. It is apparent from the optimized parameters that **TS56b** is a late transition state, whereas in **TS56d** and **TS56e**, the interaction between iron and the oxygen atom is already present in the transition structure, albeit attenuated with respect to the corresponding product.

Consistent with this onset of intramolecular bonding, the resulting activation barriers for these derivatives are lower by ca. 2 kcal/mol, as compared to that in the parent (see $\Delta E^‡$ values in Table 2). After zero-point correction, a decrease of the barrier of about 1 kcal/mol remains ($\Delta E^‡$ + ZPE values). From this result one can predict that carbonyl and silyl substituents at the Cp ring should increase the catalytic activity noticeably.[34] Accelerations of reactions at transition metal centers by reversible coordination (or "anchimeric assistance") of ancillary ligands are long known[35] and have led to the concept of hemilabile ligands.[36]

When the estimated free activation energies $\Delta G^‡$ are compared, that starting from the parent **5a** is lower than those involving **TS56b**, **TS56d**, and **TS56e** (Table 2). This is because entropy lowers the dissociation energy in **5a** more strongly (due to the increase in particle number) than it does for the activation barriers (since the particles are not yet fully released). However, as will be detailed in section 3, when the real phosphine PPh_3 is employed, H_2 dissociation is an activated process also for the parent complex with X = H. Consequently, the apparent entropic stabilization of this process will be much smaller than that for the model compound **5a**. It is to be expected that the energetic lowering of the activation barriers on going from **5a** to **5b**, **5d**, **5e** will also transpire to the actual, free energy barriers $\Delta G^‡$ of the real system.

No intramolecular interaction like those discussed above was found in the other substituted dissociation products, **6c**, **6f**, and **6g** (because the structures are unremarkable, they are not included in Figure 4). As with the parent system, H_2 dissociation from **5c**, **5f**, and

(34) In the case of the acetyl derivative we have also located the transition state for SiH_4 uptake by **6d**, **TS62d** (see coordinates in Supporting Information), which was found lower in energy than **TS56d** by 4.5 kcal/mol (ΔE + ZPE level, ΔG 2.5 kcal/mol), thus making sure that it is indeed H_2 dissociation from **5d** that is the rate-limiting step.

(35) E.g.: (a) Miller, E. M.; Shaw, B. L. *J. Chem. Soc., Dalton Trans.* **1974**, 480−485. (b) Chauby, V.; Daran, J.-C.; Serra-Le Berre, C.; Malbosc, F.; Kalck, P.; Gonzalez, O. D.; Haslam, C. E.; Haynes, A. *Inorg. Chem.* **2002**, *41*, 3280−3290. For a recent computational prediction see ref 39c.

(36) Review: Braunstein, P.; Naud, F. *Angew. Chem., Int. Ed.* **2001**, *40*, 680−699.

5g proceeds without extra activation on the PES,[29] and the barriers for this process are thus equal to the respective reaction energies. The latter is significantly smaller than that for the parent in the case of X = NMe_2 (by ca. 6 kcal/mol, both for $\Delta\Delta E$ + ZPE and $\Delta\Delta G$ values, Table 2) and X = Cl (by ca. 3 kcal/mol). This lowering of the barrier can be rationalized by the π-donating capabilities of these ligands, in particular for the amino group, which makes the Cp ligand more electron-rich (more basic), resulting in a better stabilization of the electron-deficient iron center. Thus, we can predict that amino substituents at the Cp ring should produce particularly active catalysts for silane alcoholysis. Interestingly, the attachment of a π-acceptor without the capability of hemilabile coordination also results in a lowering of the dissociation energy (by less than 1 kcal/mol for X = CN, Table 2). This result is more difficult to rationalize; it is possibly the intramolecular electrostatic interaction between the negatively charged CN group and the positively charged metal center that compensates for the destabilization of **6f** due to the reduced basicity of the Cp ligand.

These results indicate that substitution of a Cp hydrogen atom with the substituents under consideration should increase the catalytic activity. Interestingly, the corresponding substitutions in the actual catalyst precursors that have been realized to date lead to a deshielding of the ^{57}Fe nucleus (**1A**−**D**, see Scheme 2).[33] We were thus interested to see if this system could be another example of an NMR/reactivity correlation. For a number of catalytic[37] and stoichiometric[38] reactions at transition metal centers it has been possible to correlate reactivities or catalytic activities with the chemical shifts of the metal. When such a correlation is established within a series of closely related compounds, it could be possible, for instance, to select prospective catalysts on the basis of their NMR spectra. A few such correlations have been rationalized or predicted computationally.[39] When the computed barriers $\Delta E^{\ddagger}$ from Table 2 are plotted against the experimental $\delta(^{57}\text{Fe})$ values (crosses in Figure 5), no good correlation is obtained. When, on the other hand, the ^{57}Fe chemical shifts are computed for the model precursors **1a**−**g** (Table 2),[40] there is a loose trend with the computed barriers (black circles in Figure 5). Thus, the theoretical results appear to be consistent with each other and suggest the possibility of an NMR/reactivity correlation, but only for the model system. The transferability of this correlation to the real catalyst (i.e., the correlation between observed chemical shifts and reactivities) cannot be predicted with confidence. What can be predicted with confidence, however, is that the electron-withdrawing and -releasing substituents at the Cp ring should produce more active catalysts.

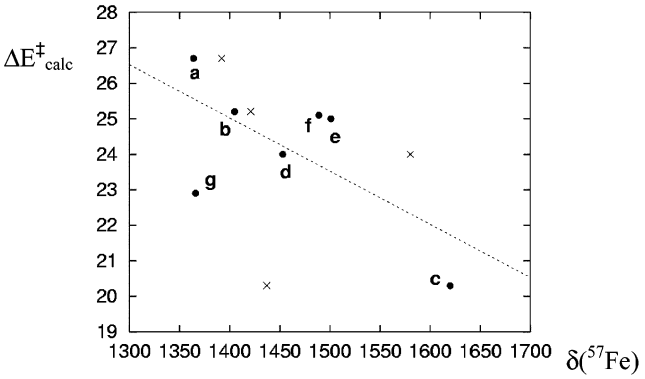

Figure 5. Correlation of the BP86/AE1 computed H_2-dissociation barriers from Table 2 [kcal/mol] with ^{57}Fe chemical shifts from experiment (×) and computed for the corresponding model complexes with PH_3 (●), including a linear regression for the latter (dotted line).

Table 3. Relative Energies (kcal/mol, BP86/AE1′ Level) of Stationary Points in Catalytic Silane Alcoholysis at the Real Catalytic Center (PPh_3 as Phosphine); {Fe} = [Fe(Cp)(CO)(PPh_3)]$^+$

complex	ΔE	ΔE+ZPE[a]	ΔH^b	ΔG^b
{Fe}(SiH_4) (**7**) + SiH_4 + MeOH	0.0	0.0	0.0	0.0
{Fe}($HSiH_3$···OHMe) (**8**) + SiH_4	−6.9	−5.4	−5.1	4.4
Fe(Cp)(CO)(PPh_3)H (**9**) + SiH_4 + MeO(H)SiH_3^+	25.3	25.2	25.0	23.5
{Fe}(SiH_4)(HOMe)‡ (**TS710a**) + SiH_4	8.7	9.7	9.3	20.9
{Fe}(H_2) (**10a**) + $MeOSiH_3$ + SiH_4	−12.1	−13.5	−14.3	−13.7
{Fe}(H_2)(SiH_4)‡ (**TS10a7**) + $MeOSiH_3$	13.3	9.0	10.6	12.3
{Fe} (**11a**) + H_2 + $MeOSiH_3$ + SiH_4	2.5	−2.9	−1.6	−10.5
{Fe}(H_2) (**TS1**) + $MeOSiH_3$ + SiH_4	12.4	8.1	8.7	6.3

[a] Including zero-point energies. [b] Thermodynamic corrections at 300 K from BP86/AE1′ harmonic frequencies.

3. The Real Catalytic Center. It is known that PH_3 is not very well suited to model steric and electronic properties of actual, bulky phosphines used in transition metal chemistry.[41] To assess the effect of the phosphine, and as a first step toward the description of the real system, we have extended our study to the real catalytic center with R′ = Ph. First, the stationary points depicted in Figures 1−3 were reoptimized at the BP86/AE1′ level using PPh_3 instead of PH_3. The corresponding energies are collected in Table 3. The evolution of the relative energies along the reaction coordinate is sketched in Figure 6 (black lines) and contrasted with the results for the model catalyst (gray lines).

Inspection of the data in Tables 1 and 3 or of Figure 6 reveals mostly quantitative changes upon going from R′ = H to Ph, and most of the qualitative conclusions from the preceding section can be transferred to the real catalyst. Specifically, as with the smaller model, single-step formation of the H_2 complex [Fe(Cp)(CO)(PPh_3)(H_2)]$^+$ (**10a**) is favored over the sequential pathway via

(37) (a) Bönnemann, H.; Brijoux, W.; Brinkmann, R.; Meurers, W.; Mynott, R.; von Philipsborn, W.; Egolf, T. *J. Organomet. Chem.* **1984**, *272*, 231. (b) Fornika, R.; Görls, H.; Seeman, B.; Leitner, W. *J. Chem. Soc., Chem. Commun* **1995**, 1479−1480.

(38) E.g.: (a) DeShong, P.; Slough, G. A.; Sidler, D. R.; Rybczynski, P. J.; von Philipsborn, W.; Kunz, R. W.; Bursten, B. E.; Clayton, T. W. J. *Organometallics* **1989**, *8*, 1381−1388. (b) Koller, M.; von Philipsborn, W. J. *Organometallics* **1992**, *11*, 467−468. Review: (c) von Philipsborn, W. *Chem. Soc. Rev.* 1999, 95−106.

(39) (a) Bühl, M. *Organometallics* **1997**, *16*, 261−267. (b) Bühl, M. *Angew. Chem. Int. Ed.* **1998**, *37*, 142−144. (c) Bühl, M. *Organometallics* **1999**, *18*, 4894−4896.

(40) The comparison of the computed δ values with experiment is complicated by the fact that in each case several rotamers about the Fe−Cp axis exist, which are within a few kcal/mol of each other, and for which the computed magnetic shieldings can cover a range of up to 200 ppm (in Table 2, the δ values of the most stable isomers are given).

(41) See for instance: Senn, H.-M.; Deubel, D. V.; Blöchl, P. E.; Togni, A.; Frenking, G. *J. Mol. Struct. (THEOCHEM)* **2000**, *506*, 233−242.

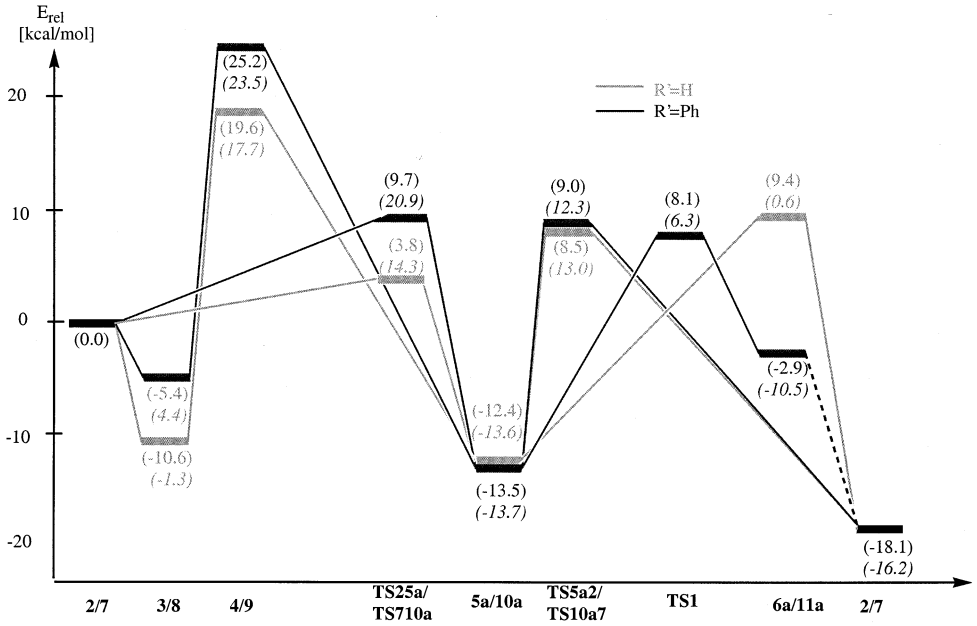

Figure 6. Schematic potential energy surface for catalytic silane alcoholysis: (gray) model catalyst (R′ = H, BP86/AE1 level); (black) real catalyst (R′ = Ph, BP86/AE1′ level); (in parentheses) relative energies including zero-point correction.

the monohydride intermediate Fe(Cp)(CO)(PPh_3)(H) (**9**). Likewise, dissociative displacement of the H_2 ligand in **10a** appears to be much more favorable than associative substitution via **TS10a7**.[42] In fact, the dissociation energy via [Fe(Cp)(CO)(PPh_3)]$^+$ (**11a**),

10a → **11a** + H_2,

ΔE + ZPE = 10.6 kcal/mol (ΔG = 3.2 kcal/mol) (8)

appears to be conspicuously small when compared to the value for the model catalyst, 21.8 kcal/mol (eq 7). Inspection of the optimized structure of **11a** (Figure 7) affords a ready explanation for this low value of the dissociation energy: As with some of the Cp-substituted derivatives discussed in the preceding section, **11a** is stabilized by an intramolecular interaction between the iron center and one of the phenyl groups. In the smaller model complex **6a**, no such saturation of the vacant coordination site at iron is possible.The interaction in **11a** leads to notable distortions in the coordination geometry of the phosphine: The lone pair at phosphorus, assumed to lie on the line forming three equal angles with the adjacent ipso-C atoms, is tilted away from Fe by more than 40°. This tilt allows the metal to interact with both ipso and ortho C atoms (Fe···C distances 2.28 and 2.41 Å, respectively). The phenyl ring is thus approaching the Fe center in a η^2 fashion, giving rise to a noticeable alternation in the remaining C−C bond lengths (between 1.392 and 1.436 Å). This coordination mode is reminiscent of that in η^3-bonded triphenylmethylmetal complexes[43] and has actually been already observed for PPh_3 bound to a transition metal.[44]

In contrast to the model dihydrogen complex **5a**, H_2 dissociation from **10a** has to pass an additional barrier on the PES. After construction of a reaction path by successive elongation of the Fe−H_2 distance in **10a**, a true transition structure could be located (**TS1**, Figure 7). On this path, the phenyl ring that is closest to the dissociating H_2 ligand eventually coordinates to iron, and the resulting barrier is 21.6 kcal/mol. This value is comparable to the H_2 dissociation energy in **5a**, 21.8 kcal/mol (see differences in corresponding ΔE + ZPE values in Tables 1 and 3 or Figure 6), suggesting that the Fe···H_2 contact in **TS1** is all but broken before

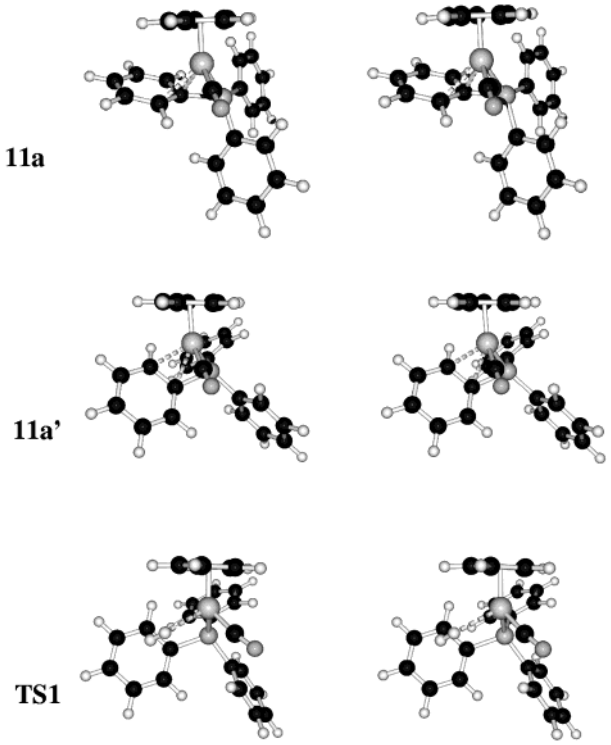

Figure 7. (Top) Complex **11a** with intramolecular Ph coordination. (Middle) Isomeric complex **11a′** with interaction with the other ortho carbon. (Bottom) Transition state **TS1** for H_2 dissociation leading to **11a′**. Stereoviews of the RI-BP86/AE1 optimized structures are shown in each case.

(42) "Dissociative" and "associative" mechanisms are the same as discussed for the model system; that is, PPh_3-based **TS10a7** (not shown) corresponds to the PH_3-derivative **TS5a2** in Figure 2.

stabilization due to the interaction with the phenyl group can take over. As with the model carbonyl derivative discussed in the preceding section, the estimated free energy of activation is higher in the agostic system via **TS1** (ΔG = 20.0 kcal/mol) than in the "barrierless"[29] model system via **6a** (ΔG = 14.2 kcal/mol). **TS1** does not lead directly to **11a** but to the related,[45] slightly less stable complex **11a′**,[46] which can either rearrange to **11a**[47] or react directly with fresh silane.

Subsequently, we were searching for a transition state[46] where a phenyl moiety in anti position to the H_2 leaving group would develop the coordination to the metal. In such an S_N2-like arrangement, creation of a free or nearly free coordination site could possibly be avoided. However, concomitant inversion at Fe would have to take place, which is an activated process in itself.[48] Despite extensive searches, no transition state for such a "backside" attack could be located.

It thus appears that "frontside attack" via **TS1** is the preferred pathway for H_2 substitution in **10a**, which also appears to be the rate-limiting step at ambient temperature (entropic contributions bring **TS1** below the competing associative **TS10a7**, cf. ΔG values in Figure 6). We have not located the transition structure for silane addition to **11a**, assuming that it will be lower in energy than **TS1**, in analogy with the findings for the model carbonyl derivative, **TS62d** vs **TS56d**.[34]

In summary, the general reaction mechanism is transferable from the model system with PH_3 to that with PPh_3, that is, to the real catalytic center. In particular, the H_2 dissociation step is confirmed as the rate-limiting one. Is the same transferability also true for the effects of substituents at the Cp rings discussed in section 2? To address this question, full transition state optimizations would have to be performed for the corresponding derivatives of **TS1**. The large conformational space (concerning the position of the substituents at the Cp ring) would render these searches for transition structures and minima very time-consuming. Even if all relevant stationary points could be located, the significance of any single static structure would probably be quite limited, and eventually one would have to resort to a dynamical approach. Following the dynamics of the full system[49] over a sufficiently long time interval, however, would be a formidable task going beyond the scope of the present paper. For the Cp derivatives the situation is further complicated by the possibility that the ligands at the Cp ring and at the phosphine can compete for the coordination site at iron in transient **11x**. For the acetyl derivative, for instance, both possibilities are similar in energy, and phenyl coordination (**11d′** in Scheme 3) is actually computed to be more favorable than carbonyl contact (**11d**) by 1.7 kcal/mol at the RI-BP86/AE1 level. It is therefore unclear at this point to what extent the lowering of the rate-determining barrier in the model system **5d** (which originates from the interaction between iron and the carbonyl group, see preceding section) would come to the fore in the real catalyst. The prediction that π-donor substituents at the Cp ring, such as amino groups, should increase the catalytic activity, however, is not affected by this argument. If an NMR/reactivity correlation would exist for this subset of derivatives, one could select prospective target catalysts based on corresponding trends in $\delta(^{57}Fe)$ values from the literature. For instance, N-silylation of *N*-ferrocenylamine affords a deshielding of the ^{57}Fe nucleus.[32b] Complexes of type **1** with an $-N(SiR_3)$ motif at the Cp ring could thus be promising catalyst precursors for silane alcoholysis.

Scheme 3

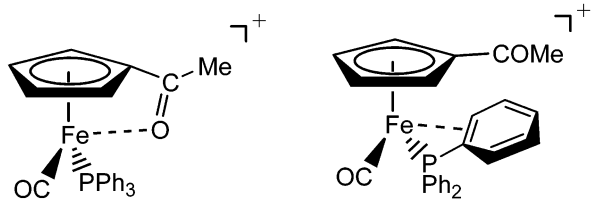

11d **11d'**

Finally, the participation of a phenyl group from the phosphine in the rate-determining step can open further possibilities for the tailoring of catalyst properties. It is conceivable, for instance, that the strength of the intramolecular coordination as in **11a** can be fine-tuned by attaching appropriate substituents to the phenyl groups of the phosphine.

Conclusions

We have presented a density functional study of the mechanism of catalytic silane alcoholysis at a $[Fe(Cp)(CO)(PR'_3)]^+$ center. For both the model and the more realistic system with PH_3 and PPh_3 ligands, respectively, a detailed catalytic cycle has been characterized. The reaction path involves the free cationic center and its complexes with either silane or H_2, consistent with the mechanism deduced from detailed NMR spectroscopic studies. Additional insights are obtained from the computations regarding the participation of the high-lying, neutral hydride complex in the catalytic cycle and regarding the dissociative nature of the H_2 replacement

(43) For transition metal complexes with this moiety see: (a) Sonoda, A.; Bailey, P. M.; Maitlis, P. M. *J. Chem. Soc., Dalton Trans.* **1979**, 346−350. (b) Crocker, L. S.; Mattson, B. M.; Heinekey, D. M.; Schulte, G. K. *Inorg. Chem.* **1988**, *27*, 3722−3725. (c) Pasynkiewicz, S.; Pietrzykowski, A.; Bukowska, L.; Słupecki, K.; Jierzykiewicz, L. B.; Urbańcyk-Lipkowska, Z. *J. Organomet. Chem.* **2000**, *604*, 241−247.

(44) $[Mn(Cp)(PPh_3)(CO)_2]^+$: Cheng, T.-Y.; Szalda, D. J.; Bullock, R. M. J. *Chem. Commun.* **1999**, 1629−1630.

(45) **11a** and **11a′** differ in the stereochemistry at the (pseudoaxially symmetric) phosphine center. The entries in Table 3 correspond to the orientation of the phenyl groups of the phosphine as in **11a′**; very similar relative energies are expected for the diastereotopic set with reversed stereochemistry (inverted propeller configuration) at phosphorous.

(46) These computations were effected with the more approximate, but faster RI-BP86/AE1 method.

(47) Inversion of the propeller configuration of free and coordinated PPh_3 ligands can occur with relatively small barriers, see for instance: (a) Costello, J. F.; Davies, S. G. *J. Chem. Soc., Perkin Trans. 2* **1998**, 1683−1689. (b) Ayscough, A. P.; Costello, J. F.; Davies, S. G. *Tetrahedron: Asymmetry* **2001**, *12*, 1621−1624.

(48) For **6a**, for instance, inversion at Fe via a C_s-symmetric transition structure costs 4.1 kcal/mol at the BP86/AE1 level.

(49) Since the interaction between metal and remote ligands is of paramount importance, methods based on empirical force fields or on suitable combination of quantum-mechanical and molecular mechanical descriptions (for a review of applications to transition metal systems see, e.g.: Maseras, F. *Chem. Commun.* **2000**, 1821−1827) cannot be applied here or are only of limited use.

by silane. The latter step is indicated to be the rate-determining one, in accordance with the interpretation of experimental results.

For the model system with PH_3, we have studied how derivatization of the Cp ring would affect the barrier of this limiting step and, thus, the overall catalytic activity. Both electron-withdrawing and -releasing substituents have been shown to lower this barrier and should thus produce more active catalysts. Derivatives with π-donors such as amino groups are predicted to be particularly effective for this purpose.

The crucial barrier can be affected by reversible intramolecular coordination of remote substituents (or hemilabile ligands) in the free $[Fe(C_5H_4X)(CO)(PR'_3)]^+$ center. The situation is complicated by a possible competition between coordination of X and of R′. Nonetheless, the predicted feasibility of an intramolecular coordination of a phenyl group of PPh_3, and its consequence on the rate-limiting barrier, opens further possibilities for the tailoring of catalyst properties. The latter should be achievable by way of suitable modifications of the phosphine.

In summary, we have shown that the silane-alcoholysis catalyst derived from $Fe(Cp)(CO)(PPh_3)Me$ shows promise for further development. We have suggested specific modifications how the catalytic activities of such complexes can be enhanced, predictions that are readily amenable to experimental verification. If suitable substituents can be found that also suppress undesirable side reactions (which were not the topic of this study), the design of new, versatile catalysts for silane alcoholysis appears to be within reach.

Acknowledgment. We wish to thank Prof. W. Thiel, the MPI für Kohlenforschung, and the Deutsche Forschungsgemeinschaft for support, the latter also for a Heisenberg fellowship for M.B. Computations were performed on Compaq XP1000 and ES40 workstations at the MPI Mülheim.

Supporting Information Available: Cartesian coordinates of all iron complexes **2**−**11** in *xyz* format. This material is available free of charge via the Internet at http://pubs.acs.org.

OM020890M